Thermodynamics Behavior of Germanium During Equilibrium Reactions between FeO_x-CaO-SiO_2-MgO Slag and Molten Copper

M.A.H. SHUVA, M.A. RHAMDHANI, G.A. BROOKS, S. MASOOD, and M.A. REUTER

The distribution ratio of germanium (Ge), $L_{Ge}^{s/m}$ during equilibrium reactions between magnesia-saturated FeO_x-CaO-SiO_2 (FCS) slag and molten copper has been measured under oxygen partial pressures from 10^{-10} to 10^{-7} atm and at temperatures 1473 to 1623 K (1200 to 1350 °C). It was observed that the Ge distribution ratio increases with increasing oxygen partial pressure, and with decreasing temperature. It was also observed that the distribution ratio is strongly dependent on slag basicity. The distribution ratio was observed to increase with increasing optical basicity. At fixed CaO concentration in the slag, the distribution ratio was found to increase with increasing Fe/SiO_2 ratio, tending to a plateau at $L_{Ge}^{s/m} = 0.8$. This behavior is consistent with the assessment of ionic bond fraction carried out in this study, and suggested the acidic nature of germanium oxide (GeO_2) in the slag system studied. The characterisation results of the quenched slag suggested that Ge is present in the FeO_x-CaO-SiO_2-MgO slag predominantly as GeO_2. At 1573 K (1300 °C) and $p_{O_2} = 10^{-8}$ atm, the activity coefficient of GeO_2 in the slag was calculated to be in the range of 0.24 to 1.50. The results from the current study suggested that less-basic slag, high operating temperature, and low oxygen partial pressure promote a low Ge distribution ratio. These conditions are desired for maximizing Ge recovery, for example, during pyrometallurgical processing of Ge-containing e-waste through secondary copper smelting. Overall, the thermodynamics data generated from this study can be used for process modeling purposes for improving recovery of Ge in primary and secondary copper smelting processes.

DOI: 10.1007/s11663-016-0759-x

I. INTRODUCTION

GERMANIUM (Ge) is a lustrous, grayish-white, brittle, and scarce metalloid with a concentration in the earth's crust of about 1.6 ppm.[1–3] The average concentration of Ge in sphalerite ((Zn,Fe)S) ores is up to 0.3 mass pct. The main route for Ge production is through refining process of zinc, where Ge is recovered from zinc residue as a by-product.[4] This is mostly carried out in Belgium and Canada. Fly ash and flue dust produced from the combustion of certain coal can also be a source for Ge, with the highest concentration found from Hartley coal ash at Northumberland, U.K., *i.e.*, about 1.6 mass pct Ge.[2] There are a number of producers in China which recover Ge from coal fly ash and zinc ore. Russia has been increasing their Ge production from fly ash from Pavlovskoye coal deposit since the last decade.[5]

United State Geological Survey (USGS) estimated the worldwide end-use of Ge metal and reported that about 85 pct of Ge is used in fiber optics, inferred optics, polymerisation catalyst application, electronics, and solar application.[5] The primary way of Ge production only replenishes 70 pct worldwide demand, the rest is fulfilled by recycling of Ge from alternative resources including end-of-life (eol) products and electronic waste (e-waste).[5]

E-waste is a heterogeneous mixture of nonmetallic and metallic materials and it contains ferrous/nonferrous valuable metals and hazardous elements,[6,7] *e.g.*, copper (Cu), lead (Pb), iron (Fe), gold (Au), silver (Ag), tin (Sn), arsenic (As), selenium (Se), tellurium (Te), germanium (Ge), palladium (Pd), tantalum (Ta), cobalt (Co), ruthenium (Ru), gallium (Ga), and other metals. The growing demand of electrical and electronic equipment has resulted in the rapid increase in the generation rate of e-waste. For example, it has been shown that the e-waste generation in Australia is about three times than that of the municipal waste generation, while in Europe it is higher, *i.e.*, about five times.[8] One of the sustainable solution to this problem is through recycling and reprocessing of e-waste for handling the hazardous elements and for recovering the valuable metals including Ge.[9,10]

M.A.H. SHUVA, PhD Student, M.A. RHAMDHANI, Associate Professor, G.A. BROOKS, and S. MASOOD, Professors, are with the Department of Mechanical and Product Design Engineering, Swinburne University of Technology, Melbourne, VIC 3122, Australia, as well as with the Wealth from Waste Research Cluster, Melbourne, VIC 3122, Australia. Contact Email: ARhamdhani@swin.edu.au M.A. REUTER, Professor, is with the Helmholtz Institute Freiberg for Resource Technology (HZDR), Freiberg, 09599, Germany.

Manuscript submitted March 22, 2016.
Article published online July 27, 2016.

In metal recycling industries, the recovery of valuable metals from e-waste is carried out through a combination of improved traditional extractive metallurgy processes (for example, a combined pyrometallurgy, electrometallurgy, and hydrometallurgy processes).[11–13] The e-waste processing is usually embedded in base metal productions through copper, lead, and zinc productions. In the case of e-waste processing through copper production, the pyrometallurgy process is aimed to recover valuable metals from e-waste and enrich them into liquid copper (or matte) phase. At a later stage of the process, the liquid copper is electrorefined to produce high-purity copper and a by-product of copper sludge known as anode slime that contains the valuable metals. This anode slime is then processed using hydrometallurgical techniques for the separation and recovery of the valuable metals. Umicore is one of the largest recycling companies in the world which processes different industrial wastes including Ge-containing e-waste, by-products from the nonferrous industries, spent industrial catalysts, car exhaust catalysts, and printed circuit boards (PCBs).[14–16] They have established an integrated approach of smelting and refining processes for the recovery of precious and other valuable metals like Ge, Sn, Au, Ag, Pt, Te, and Se.[12,13]

Recently, there has been a growing interest to recycle and recover trace valuable metals found in e-waste (including Ge) through a secondary copper processing route, namely the black copper smelting process.[6,7] This is mainly due to the flexibility of the process in which different variety of secondary copper resources (including e-waste) can be inputted into the process. This process also can be carried out for small- to large-scale operations. Figure 1 shows the general flow sheet of the black copper smelting process. The first step of processing secondary low-grade copper resources is carried out in a reduction furnace where the black copper is produced. From this process, some metals (mainly Zn) also partition into the gaseous phase as Zn-rich fume, which can be recovered upon further processing. The typical operating conditions of this reduction process are at temperatures of 1523 K (1250 °C) to 1573 K (1300 °C) and oxygen partial pressures of 10^{-6} to 10^{-8} atm. The black copper produced is then oxidized in an oxidation furnace to oxidize Zn, Sn, and Pb into oxide fumes. This produces a higher purity copper, which is then further refined in an anode furnace (combination of oxidation and reduction depending on the composition). Alloyed copper scraps (of higher purity) can be added in the oxidation furnace or in the subsequent process in the anode furnace. Further impurities removal occurs during the process in the anode furnace. The anode copper produced is then electrorefined to produce ultrahigh-purity copper and by-product anode slime which is further processed to recover the valuable metals. The black copper that contains high impurities can also be treated using a different process route (shown in the bottom part of Figure 1). Firstly, it is leached in a leaching bath containing sulphuric acid, then the leach liquor solution is subjected to electrowinning to get high-purity copper cathode. As a by-product, leaching residue from leaching and electrowinning is subsequently processed further to recover the precious metals.

The existing processes applied in industry for recovering all valuable metals are far from optimized. This is mainly due to the limited fundamental information on the behavior of the trace valuable elements during the smelting processes. For example, it has been shown that there is a very limited data on the distribution ratio, $L_{\mathrm{M}}^{s/m}$

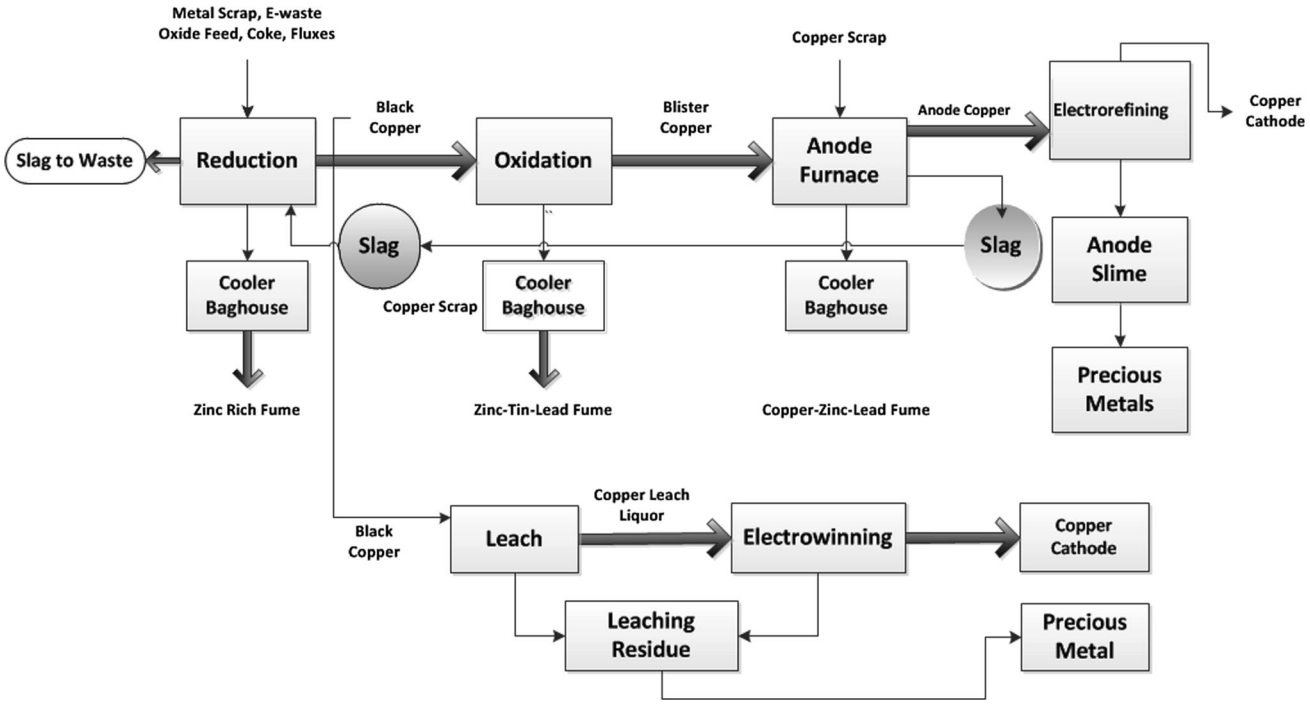

Fig. 1—Simplified flow sheet of the black copper smelter and black copper leaching.

of valuable elements on the conditions relevant to primary and secondary copper smelting.[17] There have been a number of studies on the distribution behavior of selected valuable metals in molten copper and slag under primary copper smelting processes, such as Au,[18] Pt,[19] Pb,[20] Sn,[6] In,[7,21] Se,[22] Te,[22,23] Co,[24] As,[25] and Bi.[26] However, no information and data are available in the literature on Ge distribution at conditions relevant to both primary and secondary copper smelting process.[17]

There are only two experimental studies found in the open literature on the investigation of Ge behavior during pyrometallurgical processing. Yan and Swinbourne[27] investigated the Ge distribution at conditions relevant to zinc-lead smelting process. In this study, Pb and Ge were equilibrated with $CaO-SiO_2-FeO-Al_2O_3$ slag in an alumina crucible at oxygen partial pressures of $10^{-12.5}$ to 10^{-10} atm and temperatures of 1423 K to 1523 K (1150 °C to 1250 °C). In these conditions, they found that Ge is likely to go to the slag phase and present as GeO (Ge^{2+}). They also reported that temperature and slag composition have a small effect on the Ge distribution ratio within the parameters studied. A highly reducing atmosphere was found to increase the loss of Ge into the gas phase rather than increasing the Ge concentration in the metal phase. It was also concluded in this study that there are little opportunities to reduce the Ge loss by controlling the lead smelting conditions.

Another study performed by Henao *et al.*[28] examined the distribution ratio of Ge in lead bullion and liquid slag $CaO-SiO_2-FeO-Fe_2O_3-MgO$ under oxygen partial pressures of 10^{-12} to 10^{-8} atm at 1473 K (1200 °C). Henao *et al.*[28] utilized electron probe X-ray microanalysis (EPMA) to analyze the quenched liquid slag. It was suggested that Ge was present in the slag as GeO_2 (Ge^{4+}) and that the slag composition enhances the partitioning of Ge to the lead phase. These discrepancies with the previous study of Yan and Swinbourne[27] may be attributed to the different slag system (compositions) and crucible material used in their study. Henao *et al.*[28] also carried out selected experiments at higher temperatures. However, due to excessive volatilization, Ge in the slag and metal was not detected (beyond the detection limit of EPMA technique).

The present study focuses on the investigation of distribution ratio and thermodynamics behavior of Ge in $FeO_x-CaO-SiO_2-MgO$ slag and molten copper under conditions relevant to the black copper smelting. The distribution ratio data obtained in this study are also used to calculate the activity coefficient of germanium oxide and to determine the oxidation state of germanium in the slag.

II. EXPERIMENTAL METHODOLOGY

A. *Materials Preparation*

Master slags were prepared from SiO_2 (99.5 pct purity), $CaCO_3$ (99.5 pct purity), Fe_2O_3 (99.99 pct purity), and Fe (99.9 pct purity) powder, obtained from Alfa Aesar. $CaCO_3$ was dried to remove moisture at 773 K (500 °C) for 5 hours, followed by heating at 1373 K (1100 °C) for 4 hours in a high-purity alumina tray inside a muffle furnace to produce CaO. The appropriate amount of iron, ferric oxide, silicon dioxide, and calcium oxide (calcined $CaCO_3$) targeting selected Fe/SiO_2 ratios and CaO contents were weighed and mixed in a ball mill for 36 hours. The milled powders were then transferred to a high-density magnesia crucible (OD; 48 mm, ID; 42 mm, HT; 51 mm) for melting to produce slags.

The melting of the mixtures was carried out in a vertical tube resistance furnace where the crucibles were placed in the hot zone suspended using an alumina (99.8 pct purity) rod. At the beginning, the air inside this furnace was evacuated using an external vacuum pump before backfilled with high-purity argon gas. The mixtures of powders were heated to 1573 K (1300 °C) with a heating rate of 200 °C/hour and preequilibrated for 6 hours at 1573 K (1300 °C) under controlled $CO-CO_2$ atmosphere at oxygen partial pressure $p_{O_2} = 10^{-8}$ atm. After 6 hours of equilibration time, the liquid slag was then quenched rapidly in the cool zone using high-purity argon gas to preserve the composition. The master slags were then recovered by carefully crushing the crucibles containing the slags. The slag samples were analyzed using inductively coupled plasma atomic emission spectroscopy (ICP-AES) technique to determine the final equilibrated composition. It was found that about 6.3 to 8.8 mass pct MgO is present in the slags due to the dissolution of the crucibles used for melting.

The master alloy Cu-Ge was prepared from copper flakes (99.99 pct purity, from Alfa Aesar) and germanium powder (99.99 pct purity, from Sigma-Aldrich). A mixture of copper flakes with 5 wt pct Ge was equilibrated for 6 hours in a high-density magnesia crucible (OD; 48 mm, ID; 42 mm, HT; 51 mm) inside a vertical tube resistance furnace. At the beginning the furnace was evacuated using an external vacuum pump before backfilled with high-purity argon gas. The master alloy was then heated up to 1573 K (1300 °C) with a heating rate of 200 °C/hour under high-purity argon gas. The liquid master alloy was then cooled inside the furnace using the same cooling rate. The composition of master alloy was confirmed using ICP-AES technique. It was found that approximately 1 mass pct of Ge was volatilized during the melting procedure. A trace amount of magnesium (< 0.005 mass pct) from the crucible was found in the master alloy.

B. *Experimental Apparatus, Procedure, and Conditions*

The equilibration experimental works were conducted in a vertical tube resistance furnace (Nabertherm, model: RHTV 120-300/18) which have six $MoSi_2$ heating elements and a Eurotherm automatic temperature controller was used to control the furnace temperature. The furnace was fitted with water-cooled stainless steel flanges at both ends of the tube and connected to gas lines. Prior to experiments, the temperature profile measurement and calibration were carried out using an

R-type (Pt/Pt-13 wt pct Rh) standard calibration thermocouple, to determine the hot zone and the actual temperature at locations along the length of the tube inside the furnace. The temperature was found to be accurate within ±2 K (±271 °C). The appropriate gas mixture was flown into the furnace through an inlet gas line at the bottom flange and exited through the outlet line at the top flange. Figure 2 shows the schematic diagram of the experimental apparatus used in the current study.

Two types of experiments were carried out in the current study, *i.e.*, equilibration experiment approaching from reduced and oxidized conditions, respectively. Samples with approximately 3.5 g of master slag, 2.8 g of copper, and 0.7 g of master alloy (Cu-3.9 mass pct Ge) were used for experiments approaching equilibrium from reduced condition. For experiments approaching from oxidized condition, samples with 3.5 g of copper, 3.45 g of master slag, and 0.05 g of GeO_2 (99.999 pct, purity from Alfa Aesar) were used. These mixtures were placed in high-density magnesia crucibles (OD 18 mm, ID 14 mm, HT 30 mm). It was expected that some Ge and its associated compounds volatilized during equilibration experiments. There are not many data available on the vapor pressure of Ge and Ge oxides. Hultgren *et al.*[29] reported a vapor pressure of Ge (g) over Ge (s) of 1.02×10^{-4} Pa at 1200 K (927 °C). Swamy *et al.*,[30] interpolated data from Davydov,[31] and reported a vapor pressure of GeO_2 (g) over GeO_2 (s) of 1×10^2 Pa at 1473 K (1200 °C).

To reduce the Ge or GeO_2 losses, the crucible containing the sample was placed on top of a bed of alumina powder and covered with a bigger high-purity alumina crucible in an upside-down position, as shown in Figure 2. This technique to reduce volatilization has been successfully demonstrated by Louey *et al.*[32] This assembly was then placed in the hot zone inside the furnace and supported with a high-purity alumina pedestal rod. For the equilibration experiments, initially the furnace chamber was evacuated using a vacuum pump at room temperature before backfilled with high-purity argon gas. The furnace then heated up to the desired temperature before CO_2-CO gas mixture was flown into the furnace chamber. The desired oxygen partial pressure in the furnace at a particular temperature was achieved by flowing appropriate ratio of CO-CO_2 gas mixture considering Eq. [1] which was reported by Yazawa and Takeda.[33] The individual gas flow of CO_2 and CO was regulated using a digital mass flow controller (DFC; Aalborg, USA) which was precalibrated with a manual gas flow meter. The purity of CO_2 and CO gases used in the experiment was 99.995 pct and 99.5 pct, respectively. The gas mixture was introduced from the bottom of the furnace to minimize the effect of thermal segregation, and oxygen back diffusion from the air into the furnace was prevented using a gas bubbler before release to the exit line.

$$\log p_{O_2} = 2\log\left(\frac{CO_2}{CO}\right) - \frac{29,510}{T} + 9.05. \qquad [1]$$

The overall flow rate of gas used in each experiment was 400 mL/min. To confirm the oxygen partial pressure, a $SIRO_2$ C700+ zirconia ceramic electrolyte oxygen sensor (Ceramic Oxide Fabricators, Australia) was used to measure the actual oxygen partial pressure in the furnace as shown in Table I. After the equilibrium time was achieved, the experiment was terminated by purging a high-purity argon gas for 5 minutes and the crucible system was immediately quenched by lowering it to the cool zone at the bottom of the furnace. Once

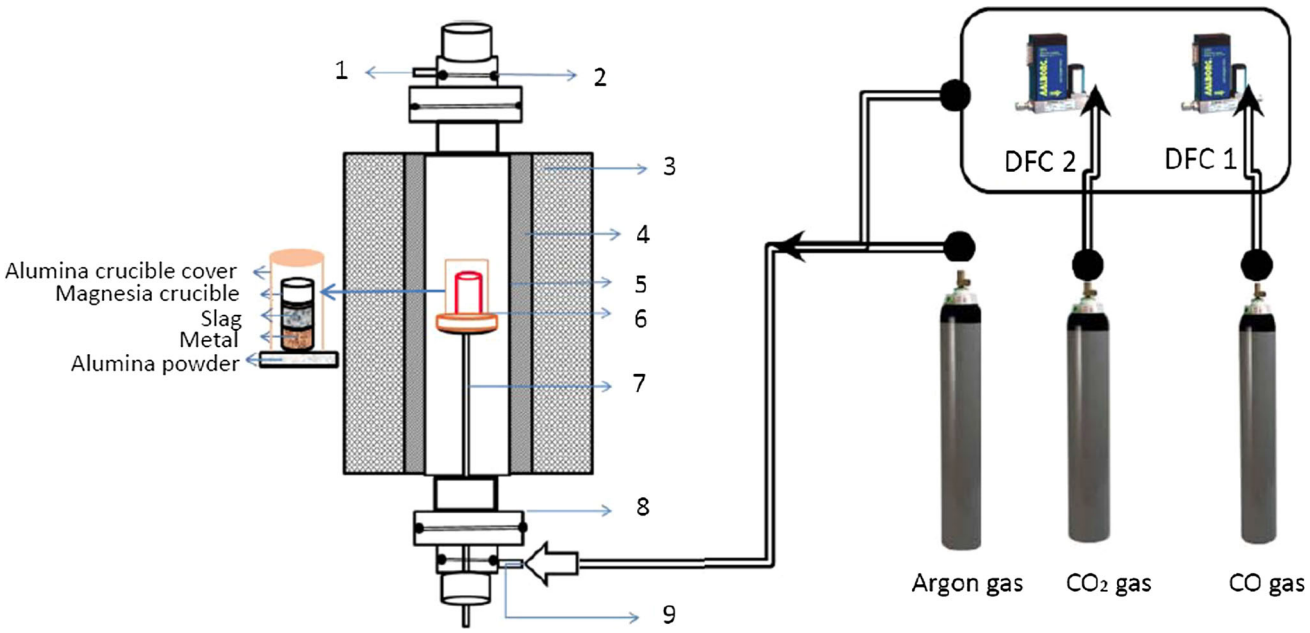

Fig. 2—Schematic of the experimental apparatus: tube furnace and gas arrangement used in the experiment: (1) gas outlet, (2) silicone O-ring, (3) $MoSi_2$ eating element, (4) alumina tube, (5) mullite tube, (6) magnesia crucible, (7) alumina pedestal, (8) water cooled flange, (9) gas inlet.

Table I. Experimental Conditions Studied

Temperature (K) (°C)	1473 (1200), 1523 (1250), 1573 (1300), 1623 (1350)			
Slag Composition (mass pct)	Fe_{Total}	SiO_2	CaO	MgO
	37.3	35.3	5.59	6.3
	27.4	33.9	9.72	6.78
	32.8	33.1	9.88	6.49
	37.9	32.8	9.80	6.51
	41.8	31.9	9.95	6.35
	33.4	33.6	14.5	7.52
	31.1	32.6	14.5	7.83
	30.7	31.3	19.4	8.78
Oxygen Partial Pressure (atm)	Target p_{O_2}	Temperature [K (°C)]		Measured p_{O_2} ‡
	10^{-8}	1473 (1200)		9.64×10^{-9}
	10^{-8}	1523 (1250)		1.03×10^{-8}
	10^{-8}	1573 (1300)		9.47×10^{-9}
	10^{-8}	1623 (1350)		9.85×10^{-9}
	10^{-7}	1573 (1300)		9.46×10^{-8}
	10^{-9}	1573 (1300)		9.34×10^{-10}
	10^{-10}	1573 (1300)		9.48×10^{-11}

‡ Measured EMF using $SIRO_2$ sensor.

cooled down, the crucible system was collected and it was carefully crushed and the copper and slag were separated by physical means. In the current study, the effect of temperature, oxygen partial pressure, and the different slag composition were investigated. Table I shows the experimental conditions studied.

C. *Chemical Analysis and Characterization*

After the slag and the metal samples were separated, they were fused using sodium peroxide and dissolved in hydrochloric and nitric acids. The solutions were then analyzed using ICP-AES (inductively coupled plasma—atomic emission spectrometry) technique (Varian 730 ES: ICP-AES) to determine the bulk chemical compositions. The slag samples were also characterized using XRD (X-ray diffraction) technique (AXS-D8, Bruker) equipped with Cu Kα (λ = 1.5406 Å) radiation target. The diffraction patterns were collected over a 2θ range from 10 to 80 deg at a step size of 0.02 deg. Raman spectrometry analyses were also carried out on selected slag samples using a Raman spectroscope (inVia, Renishaw, U.K.) equipped with a Leica microscope. The Raman spectra measurements were carried out using an excitation wavelength of 785 nm from an argon-ion laser.

III. RESULTS AND DISCUSSION

A. *Checking of Equilibrium and Determination of Minimum Equilibration Time*

The attainment of equilibrium and the time to reach this condition were investigated by carrying out equilibration experiments approaching from an opposite direction, *i.e.*, approaching from oxidized and reduced conditions. A slag having Fe/SiO_2 ratio (in weight) of 0.99 and CaO concentration of 14.5 mass pct was equilibrated with copper at oxygen partial pressure of 10^{-8} atm at 1573 K (1300 °C). It has been mentioned that some of the MgO from the crucible entered into the slag. It was predicted by FactSage thermochemical software calculation that this condition is in the liquid region of the FeO_x-CaO-SiO_2-MgO (FCS) slag system. A number of equilibration experiments were carried out with reaction time from 4 to 20 hours from both directions (approaching from oxidized and reduced conditions) to investigate the time required to reach equilibrium. Germanium is volatile in the conditions studied; to investigate the Ge loss by volatilization, mass balance coupled with bulk chemical analyses of copper and slag phase were carried out at different reaction time and the results are presented in Table II. To avoid excessive Ge volatilization and reshifting of equilibrium, it was necessary to determine the earliest time to reach equilibrium.

The data in Table II are plotted and presented in Figure 3. It can be seen that at $p_{O_2} = 10^{-8}$ atm there are no significant differences in the distribution ratio of Ge in slag and metal after 6 hours of equilibration approaching from both the oxidized and reduced conditions. It was also observed that with the increase of reaction time, more Ge is volatilized. Depending on the reaction time, about 20-55 mass pct Ge was found in copper metal, 21-49 mass pct in the slag, and 2-60 mass pct volatilized.

To investigate further the appropriate minimum equilibration time, four additional experiments at different oxygen partial pressure were carried out. One set of experiments was carried out at 1573 K (1300 °C) and $p_{O_2}10^{-10}$ atm for 6 hours equilibrium time and another set at 1573 K (1300 °C) and $p_{O_2}10^{-9}$ atm for 10 hours from both directions. It can be seen from Figure 3 that at the indicated equilibration times, it was sufficient for

Table II. Distribution of Ge Among Slag, Metal, Gas as a Function of Equilibrium Time at 1573 K (1300 °C) and $p_{O_2} = 10^{-8}$ atm with a Slag Composition of $Fe/SiO_2 = 0.96$ and Mass Pct CaO = 14.5

	Slag		Metal			
Equilibrium Time (h)	Ge Mass Pct	Distribution Pct	Ge Mass Pct	Distribution Pct	Gas Loss Pct	$L_{Ge}^{slag/metal}$
Approaching from Reduced Condition						
4	0.33	42.31	0.43	55.13	2.56	0.77
6	0.37	47.44	0.35	44.87	7.69	1.06
8	0.34	43.59	0.33	42.31	14.10	1.03
16	0.27	34.62	0.25	32.05	33.33	1.08
20	0.24	30.77	0.22	28.21	41.03	1.09
Approaching from Oxidized Condition						
4	0.55	49.19	0.44	39.36	11.45	1.25
4	0.53	47.41	0.41	36.67	15.92	1.29
8	0.49	43.83	0.43	38.46	17.71	1.14
16	0.39	34.88	0.35	31.31	33.81	1.11
20	0.23	20.57	0.22	19.68	59.75	1.05

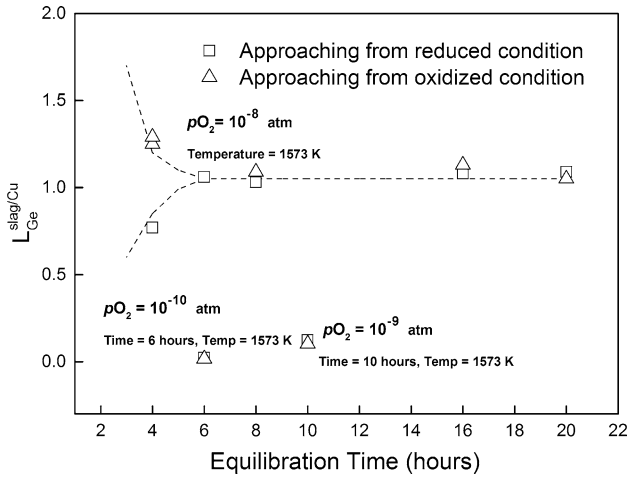

Fig. 3—Germanium distribution in FeO_x-CaO-SiO_2-MgO slag and copper metal as function of equilibration time at 1573 K (1300 °C).

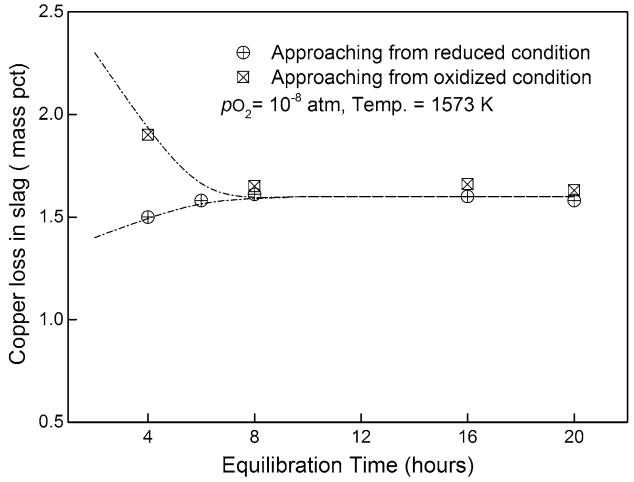

Fig. 4—Copper loss in FeO_x-CaO-SiO_2-MgO slag as a function of reaction time at 1573 K (1300 °C).

the system to reach the equilibrium state at the two oxygen partial pressures. The data in Table II also show that the Ge loss to the slag phase was smaller when the equilibrium is approached from oxidized condition. In this situation, Ge was added in the form of GeO_2 to the slag mixture at the beginning. This suggests that the Ge volatilization rate is higher when Ge is initially present in the copper phase compared to when it was present as GeO_2 or within the slag phase.

In addition to the Ge content, the Cu loss to the slag was also measured and tracked with time. Figure 4 shows the associated Cu loss to the slag as a function of time at temperature of 1573 K (1300 °C) and p_{O_2} of 10^{-8} atm. It was found that the loss of Cu to the slag is less than 2 mass pct in all experiments and levels at 1.6 mass pct at equilibrium. This finding is in agreement with Yazawa *et al.*[33–35] which reported the copper content in FCS slags to be in the range of 2 to 3 mass pct.

All the above results indicated that an equilibration time of 6 hours was sufficient for achieving equilibrium condition with minimum Ge loss to the gas phase. Therefore, further experiments were carried out using an equilibration time of 6 hours, unless otherwise stated.

B. *Effect of Oxygen Partial Pressure on the Germanium Distribution*

The effect of oxygen partial pressure on the distribution ratio of Ge, $L_{Ge}^{s/m}$, was investigated in the current study. The slag composition for this series of experiments was fixed at Fe/SiO_2 ratio of 0.96, and concentrations of CaO and MgO of 14.5 mass pct and 7.8 mass pct, respectively. At high oxygen partial pressure, magnetite formation becomes easier. To avoid the magnetite formation, the experiments were performed in the range of oxygen partial pressure between 10^{-7} and 10^{-10} atm at 1573 K (1300 °C).

The results from the experiments are given in Table III and are also plotted against oxygen partial pressure in a logarithmic form in Figure 5. For comparison, the previous published data of Ge distribution in lead smelting systems[27,28] and the prediction distribution calculated using the FactSage™ 6.4

Table III. Distribution of Ge in Slag, Metal, Gas at 1573 K (1300 °C) with a Slag Composition of $Fe/SiO_2 = 0.96$, CaO = 14.5 Mass Pct and MgO = 7.8 Mass Pct and Equilibrated for 6 h

	Slag		Metal				
log p_{O_2}	Ge Mass Pct	Distribution Pct	Ge Mass Pct	Distribution Pct	Gas Loss Pct	$L_{Ge}^{s/m}$	$\text{Log}L_{Ge}^{s/m}$
−7	0.65	83.33	0.105	13.46	3.21	6.19	0.79
−8	0.37	47.44	0.35	44.87	7.69	1.06	0.02
−9	0.08	10.26	0.63	80.77	8.97	0.13	-0.90
−10	0.014	1.79	0.73	93.58	4.63	0.02	-1.69

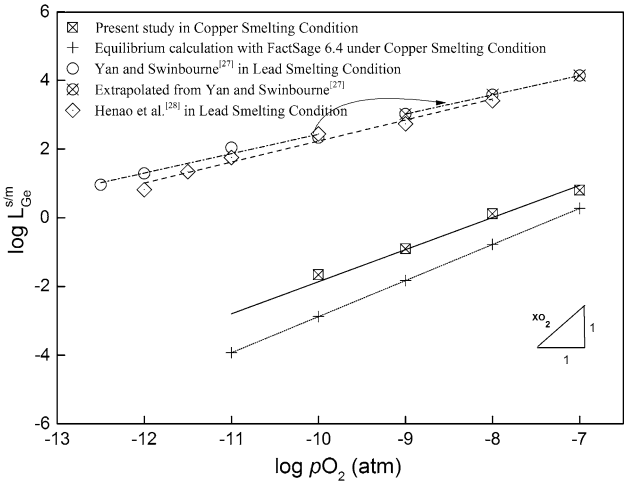

Fig. 5—Germanium distribution ratio in FeO_x-CaO-SiO_2-MgO slag and metal (copper and lead) as a function of oxygen partial pressure at 1573 K (1300 °C).

(CRCT—Thermofact and GTT Technology, Canada) for similar types of slag and alloy composition at 1573 K (1300 °C) are also presented in Figure 5. FactSage™ 6.4 is a commercial thermochemical software commonly used for multiphase gas–slag–metal equilibria calculations in both ferrous and nonferrous systems.[36] It should be noted that the slag oxide database FToxid in FactSage 6.4 and 7.0 (latest version) is not yet optimized for GeO_2-containing slags. Only the GeO_2-SiO_2 system has been evaluated over the entire composition range[37] using the data selected by Swamy *et al.*[30] for Ge-Si-O-Cl-H system. Therefore, the predicted results from FactSage shown in Figure 5 should be taken as indicative.

The distribution ratio of Ge ($L_{Ge}^{s/m}$) in slag and metal can be expressed through Eq. [2] below:

$$L_{Ge}^{s/m} = \frac{(\text{mass pctGe})_s}{[\text{mass pctGe}]_m}, \qquad [2]$$

where the subscript '*s*' denotes value in the slag and '*m*' denotes value in the metal. The distribution ratio can be presented in a different form which can provide information about the nature of the species in the slag; an approach which has been used by Takeda *et al.*[38] As a first step to investigate the nature of Ge in the slag (*e.g.*, its oxidation state), the approach of Takeda *et al.*[38] was adopted in the current study as described in the following paragraph.

Consider a general reaction for oxidation of metal as described in the following equation:

$$M + \frac{v}{2}O_2 = MO_v. \qquad [3]$$

Takeda *et al.*[38] described that the oxide in the slag can be indicated in a monocation form (*e.g.*, $MO_{0.5}$ rather than M_2O), and thus the distribution ratio can be expressed as

$$L_M^{s/m} = \frac{K(n_T)[\gamma_M^o]p_{O_2}^{v/2}}{[n_T](\gamma_{MO_v})}, \qquad [4]$$

where K is the equilibrium for Reaction in Eq. [3], n_T is the total number of moles in constituents in the relevant phases, γ_M is the activity coefficient of M in the metal, γ_{MO_v} is the activity coefficient of metal oxide MO_v in the slag, and p_{O_2} is the oxygen partial pressure. The activity coefficient of metal and oxide can be assumed to be constant if their relative concentration is very small. Therefore, the Eq. [4] can be reformulated as

$$\log L_M^{s/m} = \log B + \left(\frac{v}{2}\right)\log p_{O_2}. \qquad [5]$$

From the slope of the linear relationship between $\log L_M^{s/m}$ and $\log p_{O_2}$, the degree of oxidation of solute element $\frac{v}{2}$ in the slag can be determined. Therefore, a slope of one may indicate that the metal M is present in the slag as tetravalent M^{4+} (MO_2), while a slope of 0.5 indicates the metal present as divalent M^{2+} (MO).

Figure 5 shows that the oxygen partial pressure has a significant effect on the Ge distribution ratio. It can be seen that the distribution ratio increases with increasing oxygen partial pressure. Thus, more Ge is reported to the slag as the oxygen partial pressure is increased. The experimental data from the current study can be fitted into a single straight line. The slope was found to be close to 1, *i.e.*, 0.93. Similar line trend and gradient were observed from the FactSage prediction as shown in Figure 5. However, FactSage underpredicted the Ge distribution ratio by a factor of 10.

For comparison, previous studies on Ge distribution in a lead smelting system were also analyzed. Yan and Swinbourne[27] studied the Ge distribution ratio in a lead (Pb)-slag (FeO-CaO-SiO_2-Al_2O_3) system at much lower oxygen partial pressure (10^{-10} to $10^{-12.5}$). Their data were also plotted in Figure 5 and it can be seen that they can also be fitted in a straight line but with a smaller value of slope, *i.e.*, 0.57. They suggested in their study

that Ge was present in the slag rather as divalent Ge^{2+} (GeO). Henao *et al.*[28] reported a similar trend of the distribution ratio of Ge (with a slope of 0.61) but suggested the tetravalent oxidation state of Ge in the slag. This conclusion was based on the EPMA measurement result of Ge-containing phase in the slag carried out in their study. It should be noted that in the lead-slag systems and the conditions studied by Henao *et al.*[28] and Yan and Swinbourne[27], the Ge concentration in the metal phase was very small which is likely to have contributed to the scatter of the reported data.

To reconfirm further the oxidation nature of Ge in the slag used in the current study, further characterization that comprises of XRD and Raman spectrometry analyses were carried out on the quenched slag samples. The authors were aware that analyzing the quenched slag at room temperature is not an ideal approach, but believe that it can provide some insights on the possible nature of the slags at high temperature. The result of the XRD analysis of selected quenched slag sample is presented in Figure 6. It can be seen that there were a number of crystallized phases present in the quenched slag, namely forsterite—$(Mg_{1.8}Fe_{0.2})(SiO_4)$, fayalite—$(Mg_{0.26}Fe_{1.74})(SiO_4)$, diopside—$Ca_{0.99}(Mg_{0.64}Fe_{0.34})(Si_{1.6}Fe_{0.42})O_6$, andradite—$Ca_3Fe_2(SiO_4)_3$, copper oxide—$Cu_2O$, and germanium oxide–$GeO_2$. The same slag sample was also analyzed using a Raman spectrometry to evaluate the molecular vibration of the compounds present. Table IV shows the typical Raman vibration frequency values of the phases identified using the XRD technique[39–43] while the result of the Raman spectrometry analysis of the quenched slag is presented in Figure 7. It can be seen in Figure 7 that Raman shift spectrum confirms the presence of the forsterite, fayalite, diopside, andradite, Cu_2O, as well as GeO_2. These results further support the idea that Ge is present in the slag as tetravalent Ge^{4+} (or GeO_2).

The copper loss to the slag was also tracked in the current study. Figure 8 shows the copper loss to the slag at temperature 1573 K (1300 °C) as a function of oxygen partial pressure. The average copper content of the slag at high p_{O_2} as shown in Figure 8, is less than 2 mass pct, while at low p_{O_2}, about 1 mass pct copper is lost to the slag. Yazawa and Takeda[33] developed the following Equation[6] to estimate the copper losses to iron-silicate and calcium-silicate slags as a function of temperature and oxygen partial pressure:

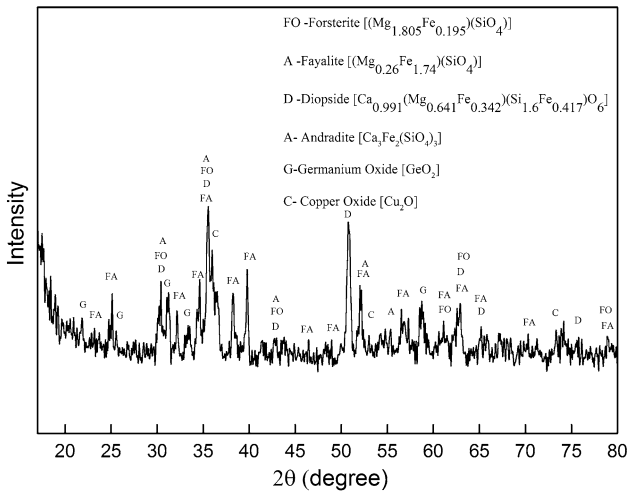

Fig. 6—XRD spectrum of a quenched FeO_x-CaO-SiO_2-MgO slag containing GeO_2 equilibrated at 1573 K (1300 °C) and $p_{O_2} = 10^{-8}$ atm for 6 h.

Table IV. Raman Vibration Frequencies of Phases Present in the Slag After Equilibrium Reaction

Phase	Vibration Frequency (cm^{-1})	References
Cu_2O	220, 661	40
GeO_2	503,593,701,973	41
Fayalite	284, 815, 841	42
Andradite	452, 576, 995	42
Forsterite	437, 610	42
Diopside	182, 392, 560	42

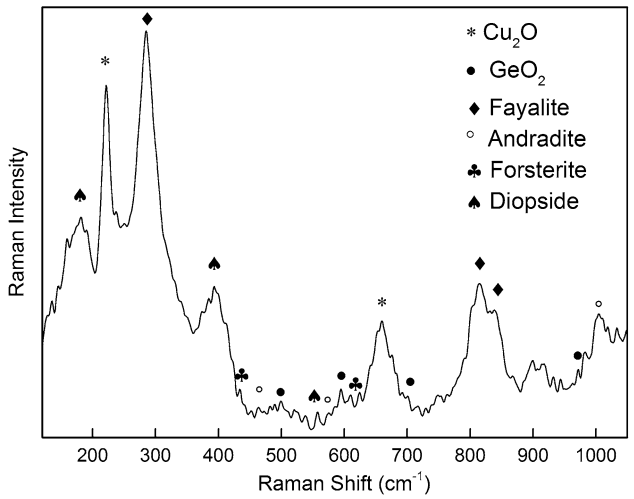

Fig. 7—Raman shift spectrum of a quenched FeO_x-CaO-SiO_2-MgO slag containing GeO_2 equilibrated at 1573 K (1300 °C) and $p_{O_2} = 10^{-8}$ atm for 6 h.

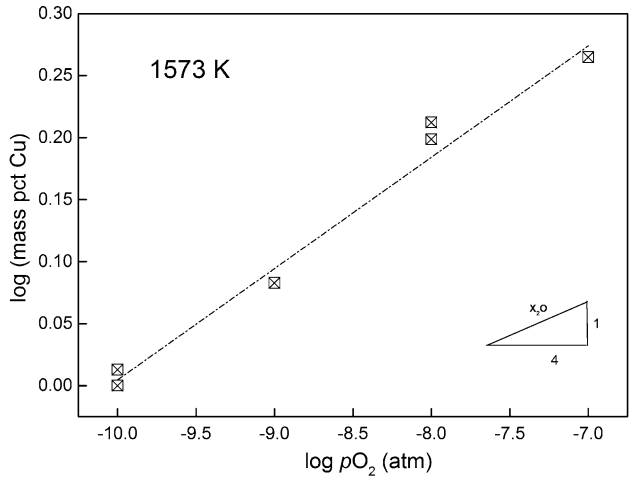

Fig. 8—Copper loss to FeO_x-CaO-SiO_2-MgO slag as a function of oxygen partial pressure at 1573 K (1300 °C).

$$\log(\text{mass pctCu}) = 0.221 \log p_{O_2} + \frac{2490}{T} + 0.455. \quad [6]$$

The current results were found to follow a similar trend to those reported by Yazawa and Takeda[33] as can be seen in Table V. The copper loss at high oxygen partial pressure ($p_{O_2} = 10^{-7}$atm) obtained in the current study, however, was much lower compared to the value predicted using Eq. [6]. It may be that different slag composition used in this study (containing MgO) contributed to the difference in the copper losses.

C. *Effect of Temperature*

The temperature dependence of Ge distribution ratio in the FeO_x-CaO-SiO_2-MgO slag system (7 mass pct MgO) and copper is shown in Figure 9. This slag contained 9.8 mass pct of CaO with Fe/SiO_2 ratio of 0.99. It can be seen that the Ge distribution ratio decreases with increasing temperature over the range 1473-1623 K (1200 °C to 1350 °C) under an oxygen potential of 10^{-8} atm. Consider a reaction in Eq. [7], a similar reaction to Eq. [3]

$$Ge_{(l)} + O_{2(g)} = GeO_{2(l)} \quad \Delta G^o = -562,000 + 180\ T\ (J/mol) \quad [7]$$

Table V. Comparison of Copper Loss to the Slag Between the Current Study and those from Yazawa and Takeda[33] at 1573 K (1300 °C)

pO_2	Mass Percentage Cu in Slag from Eq. [6]	Mass Percentage Cu in Slag in the Current Study
−10	0.7	0.97
−9	1.1	1.2
−8	1.9	1.6
−7	3.1	1.8

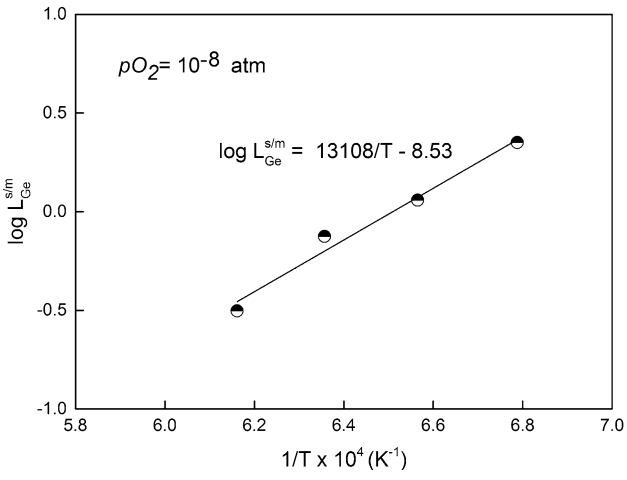

Fig. 9—The effect of temperature on the Ge distribution ratio in FeO_x-CaO-SiO_2-MgO slag and copper at $p_{O_2} = 10^{-8}$ atm equilibrated for 6 h (Fe/SiO_2 = 0.99, CaO = 9.8 mass pct).

The standard Gibbs free energy equation shown in Eq. [7] was reported by Sreedharan *et al.*[44] The value of equilibrium constant calculated using the above equation is very close to that of calculated using Factsage 6.4 thermochemical software. For example, the value of equilibrium constants of reaction in Eq. [7] at 1473 K (1200 °C), 1523 K (1250 °C), 1573 K (1300 °C), and 1623 K (1350 °C) are 33.8×10^4, 7.46×10^4, 1.82×10^4, and 4.83×10^3, respectively, as calculated using the "Reaction" module of FactSage 6.4. It can be seen here that the equilibrium constant value changes drastically with temperature. Therefore the distribution ratio would also change significantly, as expressed in Eq. [4]. It can also be seen from Figure 9 that higher amount of Ge reports to copper at higher temperatures. Moreover, the slag viscosity also decreases with increasing temperature that is also beneficial for slag separation during smelting. However, an opposite effect was observed for copper loss to the slag as shown in Figure 10. At fixed oxygen partial pressure, copper loss to the slag increases from 0.5 to 2.1 mass pct with increasing temperature. The percentage of copper loss to the FeO_x-CaO-SiO_2-MgO slag was found to be comparable to those reported in the previous studies.[22,35]

D. *Effect of Slag Composition*

The effect of slag composition, represented by the variation in the $(CaO + MgO)/SiO_2$ and Fe/SiO_2 ratios, on the Ge distribution ratio was evaluated. Basicity and acidity of a slag can be represented by the ratio of acid and basic components of the slag. In this study, the effect of the $(CaO + MgO)/SiO_2$ ratio (in mass pct), which represents the slag "basicity," on the Ge distribution ratio in FeO_x-SiO_2-CaO-MgO slag and copper is shown in Figure 11. The partitioning of Ge into the copper metal (inverse of $L_{Ge}^{s/m}$ was found to decrease with increasing addition of lime to the FeO_x-SiO_2-CaO-MgO slag. The $L_{Ge}^{s/m}$ was observed to increase up to 5 times when more CaO is added to the slag within the composition range studied. It appeared

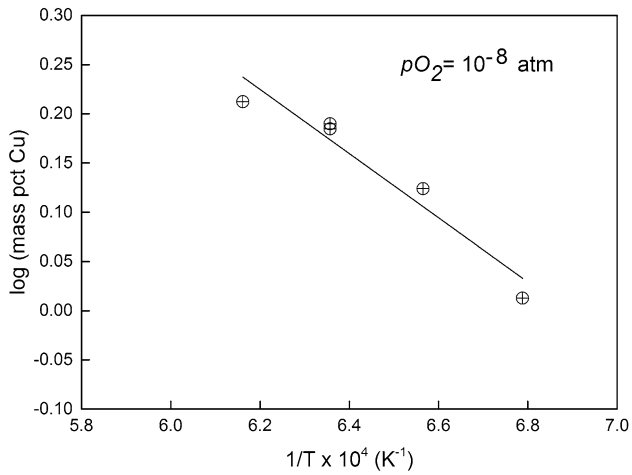

Fig. 10—Copper loss in FeO_x-CaO-SiO_2-MgO slag as a function of temperature at $p_{O_2} = 10^{-8}$ atm.

that the GeO_2 behaves as acidic oxide, as the lime content in the slag was increased resulting in a more basic slag, more Ge report into the slag. The copper loss to the FeO_x-SiO_2-CaO-MgO slag, however, appeared to not change with the variation of $(CaO + MgO)/SiO_2$ ratio at a fixed ratio of Fe/SiO_2 ~1, as shown in Figure 12. It was found that the oxide of copper behaves as a neutral oxide in the present FCS slag system. The maximum copper concentration in the slag was found to be about 1.6 mass pct, which is in good agreement with the results of Yazawa and Takeda.[33] They reported a copper concentration of less than 2 mass pct in calcium ferrite slag at $p_{O_2} = 10^{-8}$ atm and 1573 K (1300 °C). Therefore, within the range of the conditions studied, the copper loss to the slag appeared to be a function of oxygen partial pressure and temperature only.

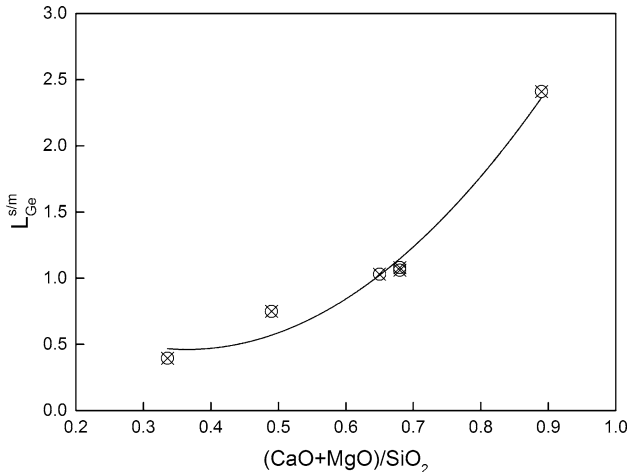

Fig. 11—The effect of $(CaO + MgO)/SiO_2$ ratio on the Ge distribution ratio in FeO_x-CaO-SiO_2-MgO slag and copper at 1573 K (1300 °C) and $p_{O_2} = 10^{-8}$ atm.

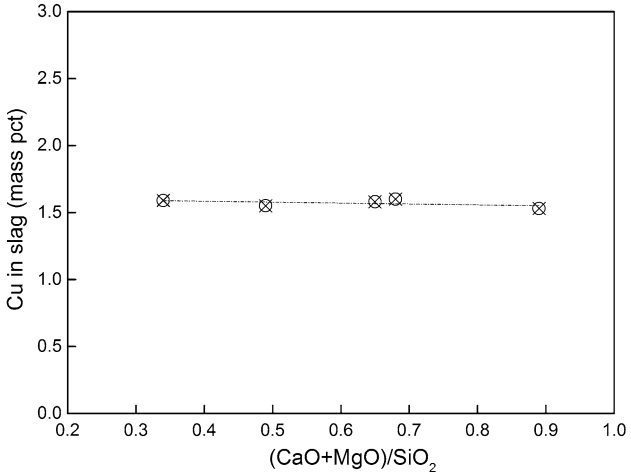

Fig. 12—The effect of $(CaO + MgO)/SiO_2$ ratio on the copper loss to FeO_x-CaO-SiO_2-MgO slag at 1573 K (1300 °C) and $p_{O_2} = 10^{-8}$ atm.

The Fe/SiO_2 ratio with fixed lime content represents the effect of slag acidity on the Ge distribution ratio, and this is shown in Figure 13. The parameter of Fe/SiO_2 ratio is also useful from the perspective of process control in industrial practice, *i.e.*, it can provide insights for balancing the appropriate amount of SiO_2 required for economical fluxing practice with low FeO activity required to avoid the formation of magnetite in the slag. The results show that the Ge distribution ratio increases with increasing Fe/SiO_2 ratio from 0.81 to 1.16. Beyond 1.16, no further increase in the Ge distribution ratio was observed. It appeared that high silica content (*i.e.*, low Fe/SiO_2 ratio) was required to keep Ge in copper. This is also in line with the observation of the effect of $(CaO + MgO)/SiO_2$ on the partitioning in Figure 12.

E. *Effect of Lime Activity on the Germanium Distribution Coefficient*

The influence of the slag "basicity" may be explained in terms of free oxygen ion. As the activity of free oxygen ion cannot be measured experimentally, it was assumed that O^{2-} ion activity can be replaced by activity of CaO at fixed temperature and oxygen partial pressure, *i.e.*, activity of CaO is proportional to O^{2-} ion. The activity of CaO in the different slag compositions studied was estimated using the FactSage 6.4 package. Figure 14 shows the linear relationship between the log of Ge distribution ratio and the log a_{CaO}. Some experimental scatter was found in the present work. It was found that as the activity of CaO in slag decreases, the Ge distribution ratio is also decreasing. Therefore, it can be suggested that, the less the O^{2-} ion present in the slag, the more likely the Ge to report to metal phase.

F. *Activity Coefficient of GeO_2 in the Slag*

The activity coefficient of GeO_2 in the slag can be calculated using Eq. [4] utilizing the information on the

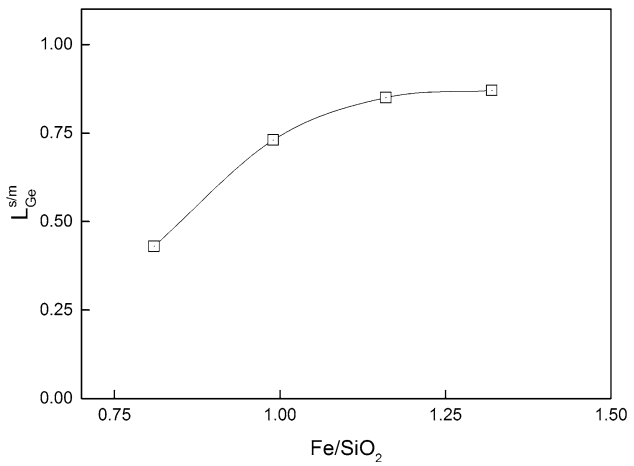

Fig. 13—The effect of Fe/SiO_2 ratio on the Ge distribution ratio in FeO_x-CaO-SiO_2-MgO slag and copper at 1573 K (1300 °C) and $p_{O_2} = 10^{-8}$ atm (CaO = 9.8 mass pct).

Ge distribution ratio obtained in this study. Upon rearranging Eq. [4], the following Eq. [8] can be derived:

$$\gamma_{MO_v} = \frac{K(n_T)\left[\gamma^o_M\right]p^{v/2}_{O_2}}{[n_T]L^{s/m}_M}. \quad [8]$$

Considering the reaction in Eq. [7], the value of equlibrium constant K can be calculated to be 1.82×10^4 at 1573 K (1300 °C). The value of $[n_T]$ is 1.57 for 100 g of copper and (n_T) is between 1.94 to 2 for 100 g of slag. The exponent "$v/2$" has a value of 1 for GeO_2 as shown in Figure 5. The value of limiting activity coefficients of Ge in copper obtained from different investigators are listed in Table VI. The values presented in the table were either taken from graph or calculated from the expressed relationship provided by the investigators.

Sodeck *et al.*[45] investigated the activity of Ge in copper in the temperature range between 1540 K (1267 °C) and 1820 K (1547 °C) using a Knudsen effusion cell and mass spectroscopy. Hager *et al.*[46] also used a Knudsen effusion cell and mass spectroscopy technique to determine the activities of Ge in Cu-Ge alloy and found a good agreement with the results of Sodeck *et al.*[45] Sigworth and Elliott[47] reported a very small value of limiting activity coefficient of Ge as minor impurities in Cu alloy, but no detailed information had been provided. Azakami and Yazawa[48] extrapolated the result of Alcock *et al.*[49] to 1473 K (1200 °C) using the following relation $T\cdot\ln\gamma^o$ = constant. Recently, Wang *et al.*[50] assessed the Cu-Ge binary system using CALPHAD method through the Thermocalc® software and very good agreement was found between the calculated and the experimental data. There is no other information on the Ge activity coefficient and the effect of temperature, particularly at 1573 K (1300 °C). The value of Ge activity coefficient used in the present study was interpolated from the finding of Hager *et al.*[46] using the extrapolation relationship used by Azakami and Yazawa.[48] The calculated Ge activity coefficient in copper and its variation with temperature, extrapolated from data in Table VI, is presented in Figure 15. It can be seen from Figure 15 that the activity coefficient of Ge in copper increases with increasing temperature.

The activity coefficients of GeO_2 in the slag were then calculated by substituting all the relevant values to the Eq. [8], and the results are listed in Table VII for different slag compositions. The effect of temperature and slag composition (represented using the $(CaO+MgO)/SiO_2$ ratio) on the GeO_2 activity coefficient are presented in Figures 16 and 17, respectively. It can be seen from Figure 16 that the activity coefficient GeO_2 in the FeO_x-CaO-SiO_2-MgO was found to decrease with increasing temperature. The reason behind the downward trend also relates to the Gibbs free energy and equilibrium constant values of reaction in Eq. [7]. Both values decrease with increasing temperature due to instability of GeO_2 at high temperature. The activity coefficient of GeO_2 in the FeO_x-SiO_2-CaO was also found to decrease with increasing $(CaO+MgO)/SiO_2$ ratio at fixed Fe/SiO_2 as shown in

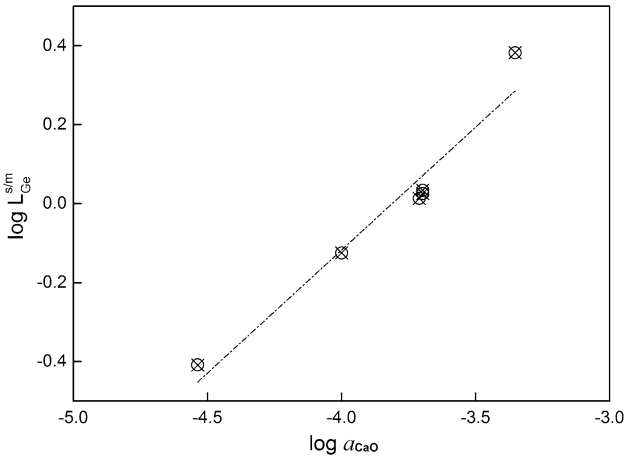

Fig. 14—Dependency of CaO activity in FeO_x-CaO-SiO_2-MgO slag on the Ge distribution ratio in slag and copper at 1573 K (1300 °C) and $p_{O_2} = 10^{-8}$ atm.

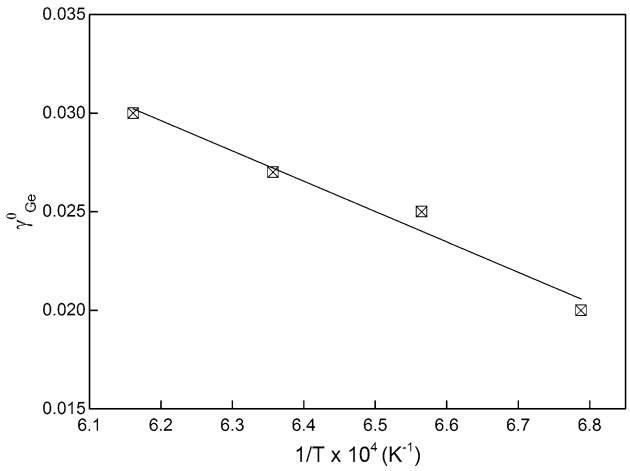

Fig. 15—Activity of Ge in copper and its variation with temperature.

Table VI. Activity Coefficient of Ge γ^o_{Ge} Copper

Temperature [K (°C)]	Sodeck *et al.*[45]	Hager *et al.*[46]	Sigworth and Elliott[47]	Azakami and Yazawa[48]
1798 K (1525 °C)	0.03‡	0.03	—	—
1473 K (1200 °C)	0.022‡	—	0.009*	0.02*

*Estimated from previous experimental data.
‡ Obtained at 1820 K (1547 °C) and 1538 K (1265 °C).

Table VII. Calculated Activity Coefficient of GeO_2 in Slag and Distribution Ratio of Ge in FeO_x-SiO_2-CaO-MgO Slag and Copper at 1573 K (1300 °C) and $p_{O_2} = 10^{-8}$ atm

	Slag Composition (Mass Pct)						
(CaO + MgO)/SiO_2	Fe_{Total}	SiO_2	CaO	MgO	n_T	$L_{Ge}^{s/m}$	γ_{GeO_2}
0.34	37.3	35.3	5.59	6.30	2.00	0.39	1.50
0.49	37.9	32.8	9.80	6.51	1.97	0.75	0.80
0.65	33.4	33.6	14.5	7.52	1.95	1.03	0.55
0.68	31.1	32.6	14.5	7.83	1.99	1.06	0.55
0.68	31.1	32.6	14.5	7.83	1.99	1.08	0.54
0.89	30.7	31.3	19.4	8.78	1.94	2.41	0.24

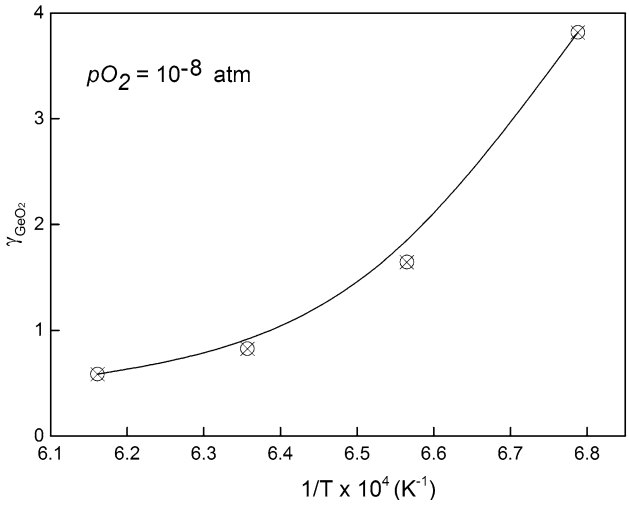

Fig. 16—The effect of temperature on the activity coefficient of GeO_2 in FeO_x-CaO-SiO_2-MgO slag and copper at $p_{O_2} = 10^{-8}$ atm (Fe/SiO_2 = 0.99, CaO = 9.8 mass pct).

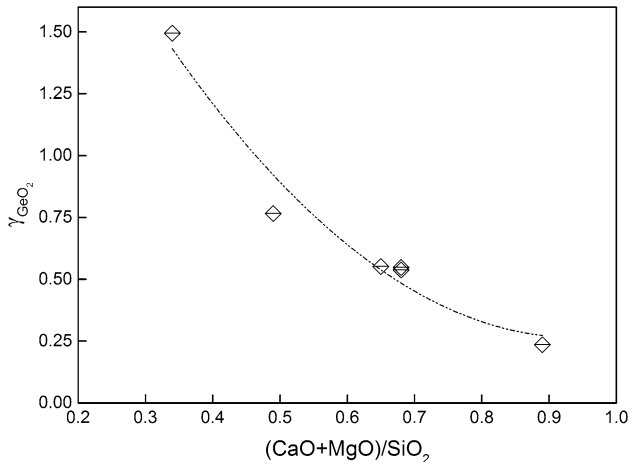

Fig. 17—The effect of (CaO + MgO)/SiO_2 ratio on the activity coefficient of GeO_2 in FeO_x-CaO-SiO_2-MgO slag and copper at 1573 K (1300 °C) and $p_{O_2} = 10^{-8}$ atm.

Figure 17. This also, again, suggests about the acidic nature of GeO_2 in the slag.

G. *Effect of Optical Basicity*

In the discussion in the preceding paragraphs, the effect of slag composition on the behavior of Ge (or GeO_2) was represented using the (CaO + MgO)/SiO_2 ratio. Another approach using an optical basicity to represent the variation of slag composition is adopted in this section. Optical basicity is a property of slag which was first suggested by Duffy and Ingram to understand the effect of metallurgical slag composition on its thermochemical properties.[51–53] The theoretical optical basicity values for pure oxides are given in Table VIII.

The optical basicity of each molten slag used in the present study as listed in Table I, was then calculated using Eq. [9]

$$\Lambda_{melt} = \frac{\sum x_i n_i \Lambda_i}{\sum x_i n_i}, \qquad [9]$$

where n_i, x_i, and Λ_i are the number of oxygen in the oxide, the mole fraction, and the theoretical optical basicity of component i, respectively. The slags used in the present study contain Fe in the form of FeO and Fe_2O_3. A special wet chemical analysis to determine the ratio of percentage of FeO and Fe_2O_3 was not carried out, rather the slags' chemistry was only determined and analyzed using ICP technique. Therefore, the equilibrium compositions of the slags (including the FeO and Fe_2O_3 concentrations) were determined by equilibrium recalculation using FactSage 6.4 considering the compositions in Table VII. The results on the recalculated equilibrium slag composition and the associated optical basicity are presented in Table IX.

Table VIII. Theoretical Optical Basicity Value for Pure Oxides

Oxide Component	Theoretical Optical Basicity
CaO	1
FeO	0.93
Fe_2O_3	0.77
SiO_2	0.48
MgO	0.78
GeO_2	0.61

The data in Table IX were plotted and presented in Figure 18. It can be seen that the distribution ratio of Ge decreases with decreasing optical basicity of the slag. It can also be seen from Figure 18 that the calculated

Table IX. Equilibrium Slag Compositions Recalculated Using FactSage 6.4, Associated Optical Basicity, Distribution Ratio of Ge, and Activity Coefficient of GeO_2 at 1573 K (1300 °C) and $p_{O_2} = 10^{-8}$ atm

Recalculated Equilibrium Slag Composition, Mass Pct							
FeO	Fe_2O_3	SiO_2	MgO	CaO	$\wedge_{melt}$	Log $L_{Ge}^{s/m}$	Log γ_{GeO_2}
40.5	10.43	36.7	6.55	5.81	0.654	-0.408	0.17
36.32	13.16	33.07	6.56	9.96	0.657	-0.125	−0.11
31.75	12.53	33.65	7.53	14.52	0.659	0.012	−0.26
30.65	12.2	33.92	8.14	15.08	0.657	0.025	−0.26
30.65	12.2	33.92	8.14	15.08	0.657	0.033	−0.27
25.98	14.81	31.15	8.73	19.31	0.664	0.382	−0.63

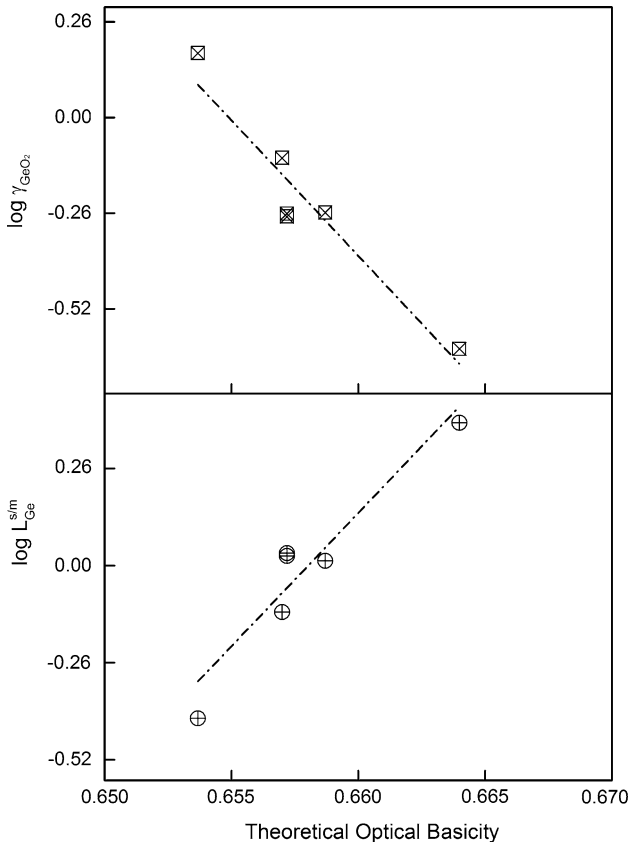

Fig. 18—The effect of optical basicity on the Ge distribution ratio and activity coefficient of GeO_2 in FeO_x-CaO-SiO_2-MgO slag at 1573 K (1300 °C) and $p_{O_2} = 10^{-8}$ atm.

activity coefficient of GeO_2 decreases with the increase of optical basicity. These observations are in line with the discussion on the effect of $(CaO + MgO)/SiO_2$ ratio on the Ge behavior in the preceding Sections.

H. *Nature of GeO_2 According to Ionic Theory*

The results from the current study suggest that the nature of GeO_2 in the slag system studied is acidic. To clarify this notion, a calculation of ionic bond fraction of GeO_2 according to the ionic theory was carried out. The ionic theory suggests that a basic slag has free O^{2-} ion. This free O^{2-} ion can easily attack an acidic oxide which means that if the nature of the minor elements oxide is acidic then the elements will tend to report to the slag. In an acid slag, there are no free O^{2-} ions but it has high capacity to incorporate basic oxide to make a more complex structure. Gilchrist *et al.*[54] categorized the acidic–basic nature of metal oxide through the ratio z/a^2. Here, z is the charge of the metal ion and a is the sum of ionic radii of two ions ($r_{cation} + r_{anion}$). They proposed the range 0.1 to 0.35 for basic oxide, 0.39 to 0.90 for intermediate oxide, and greater than 1 for acidic oxide. The ionic radii of Ge^{4+} and O^{2-} are 0.53 and 1.40 Å, respectively, and thus the value of z/a^2 for GeO_2 is 1.07 which is in the range of acidic oxide.[55] Pauling *et al.*[56] also provided a relationship of ionic bond fraction (IBF) as shown in Eq. [10] where he related the acidic–basic nature of oxide using the electronegativity of cation (x_b) and anion (x_a) of metal oxide.

$$\text{Ionic Bond Fraction (IBF)} = 1 - \exp^{-0.25(x_a - x_b)^2} \quad [10]$$

The values of x_a and x_b for GeO_2 are 3.44 and 2.01, respectively. Thus, the value of IBF for GeO_2 bond is calculated to be 0.40 which is close to Si-O bond indicated by Gilchrist *et al.*[54] All of these reconfirm the nature of GeO_2 as an acidic oxide.

IV. CONCLUSIONS

The distribution ratio and thermodynamic behavior of Ge in magnesia saturated FeO_x-CaO-SiO_2 slag and molten copper have been investigated under the conditions relevant to the copper smelting processes. The following conclusions can be drawn from the present study:

1. The Ge distribution ratio, $L_{Ge}^{s/m}$in FeO_x-CaO-SiO_2-MgO slag and molten copper was found to decrease with decreasing oxygen partial pressure at temperature 1573 K (1300 °C) for a fixed slag composition.
2. Temperature was found to have a significant effect on the Ge distribution ratio at fixed oxygen potential. At higher temperature, significant amount of Ge reported to the copper, however, copper loss to the slag was also increased.
3. At 1573 K (1300 °C) and$p_{O_2} = 10^{-8}$ atm, the Ge distribution ratio was found to be affected by the

$(CaO + MgO)/SiO_2$ ratio or optical basicity. The Fe/SiO_2 ratio was also found to affect the Ge distribution ratio but beyond 1.16 the effect is negligible.
4. The activity coefficient of GeO_2 in FeO_x-CaO-SiO_2-MgO slag was calculated and found to be in the range of 0.24 to 1.50.
5. Ge was suggested to be present in the FeO_x-CaO-SiO_2-MgO slag predominately as tetravalent Ge^{4+}, (GeO_2).
6. GeO_2 is acidic, therefore a less-basic slag (or high SiO_2 content) and higher temperature with a reducing atmosphere are recommended to decrease the Ge deportment to the slag. Higher temperature also means lower slag viscosity which promotes slag separation. Therefore, high silica content FeO_x-CaO-SiO_2-MgO slags can be used for high Ge recovery in the copper.

ACKNOWLEDGMENTS

The authors would like to acknowledge the Swinburne University Postgraduate Research Award (SUPRA) support. The authors would like to also acknowledge the support of the *Wealth from Waste Research Cluster*, a collaborative program between the Australian CSIRO (Commonwealth Scientific Industrial Research Organisation); University of Technology, Sydney; The University of Queensland, Swinburne University of Technology, Monash University and Yale University.

REFERENCES

1. J. Scoyer, G. Helian, and H.U. Wolf: *Ullmann's Encyclopaedia of Industrial Chemistry*, Wiley-VCH, Weinheim, Germany, 2001, pp. 351–63.
2. R.R. Moskalyk: *Miner. Eng.*, 2004, vol. 17, pp. 393–402.
3. R. Holl, M. Kling, and E. Schroll: *Ore Geol. Rev.*, 2007, vol. 30, pp. 145–80.
4. L. Berstein: *Geochim. Cosmochim. Acta*, 1985, vol. 49 (11), pp. 2409–22.
5. D.E. Guberman: *USGS Mineral Commodity Profile-Germanium, Open File Report 2004-1218*, USGS, 2015.
6. A. Anindya, D.R. Swinbourne, M.A. Reuter, and R.W. Matusewicz: *Miner. Process. Extr. Metall.*, 2013, vol. 122 (3), pp. 165–73.
7. A. Anindya, D.R. Swinbourne, M.A. Reuter, and R.W. Matusewicz: *Miner. Process. Extr. Metall.*, 2013, vol. 123 (1), pp. 43–52.
8. R. Widmer, H. Oswald-Krapf, and D. Sinha-Khetriwal: *Environ. Impact Assess. Rev.*, 2005, vol. 25 (5), pp. 436–58.
9. M. Reuter and I.V. Kojo: *World Metall-Erzmetall*, 2004, vol. 67 (1), pp. 5–12.
10. E. Worrell and M. Reuter: *Handbook of Recycling*, 1st ed., Elseveir, Oxford, U.K., 2014, pp. 85–94.
11. M. Firdaus, M.A. Rhamdhani, Y. Durandet, W.J. Rankin, and K. McGregor: *J. Sustain. Metall.*, 2016, DOI:10.1007/s40831-016-0045-9.
12. A. Khaliq, M.A. Rhamdhani, G.A. Brooks, and S. Masood: *Resources*, 2014, vol. 3 (1), pp. 152–79.
13. M.E. Schlesinger, M.J. King, K.C. Sole, and W.G. Davenport: *Extractive Metallurgy of Copper*, 5th ed., Elsevier, Oxford, U.K., 2011.
14. C. Hageluken: *World of Metall-Erzmetall*, 2006, vol. 59 (3), pp. 152–61.
15. J. Cui and L. Zhang: *J. Hazard. Mater.*, 2008, vol. 158, pp. 228–56.
16. J. Cui and E. Forssberg: *J. Hazard. Mater.*, 2003, vol. 99 (3), pp. 243–63.
17. M.A.H. Shuva, M.A. Rhamdhani, G.A. Brooks, S. Masood, and M.A. Reuter: *J. Clean. Prod.*, 2016, vol. 131, pp. 795–809.
18. Y.S. Han, D.R. Swinbourne, and J.H. Park: *Metall. Mater. Trans. B*, 2015, vol. 46B, pp. 2449–57.
19. K. Yamaguchi: *Proceedings. of Copper 2010*, Hamburg, 2010, vol. 3 pp. 1287–95.
20. H. Heo, S. Park, and J.H. Park: *Metall. Mater. Trans. B*, 2012, vol. 43B, pp. 1098–1105.
21. Y.S. Han and J.H. Park: *Metall. Mater. Trans. B*, 2015, vol. 46B, pp. 235–42.
22. M.D. Johnston, S. Jahanshahi, and F.J. Lincoln: *Metall. Mater. Trans. B*, 2007, vol. 38B, pp. 433–42.
23. D.R. Swinbourne, G.G. Barbanate, and A. Sheeran: *Metall. Mater. Trans. B*, 1998, vol. 9B, pp. 555–62.
24. T.S. Kho, D.R. Swinbourne, and T. Lehner: *Metall. Mater. Trans. B*, 2006, vol. 37B, pp. 209–14.
25. C. Chen and S. Jahanshahi: *Metall. Mater. Trans. B*, 2010, vol. 41B, pp. 1166–74.
26. L. Paulina, D.R. Swinbourne, and T.S. Kho: *Miner. Process. Extr Metall.*, 2013, vol. 122 (2), pp. 79–86.
27. S. Yan and D.R. Swinbourne: *Miner. Process. Extr Metall.*, 2003, vol. 112, pp. 75–80.
28. H.M. Henao, P. Hayes, E. Jak, and G.G. Richard: *Proceedings of the Lead-Zinc,* Vancouver, Canada (publ.: The Minerals, Metals & Materials Society), 2010, pp. 1145–60.
29. R. Hultgren, P.D. Desai, D.T. Hawkins, M. Gleiser, K.K. Kelly, and D. Wagram: *Selected Values of the Thermodynamic Properties of the Elements*, American Society for Metals, Metals Park, Ohio, 1973.
30. V. Swamy, S.A. Decterov, and A.D. Pelton: *Glass Sci. Technol.*, 2003, vol. 76 (2), pp. 62–70.
31. V.I. Davydov: *Zh. Neorg. Khimii*, 1957, vol. 2, pp. 1460–66.
32. R. Louey, D.R. Swinbourne, and T. Lehner: *AusIMM Proc.*, 1999, vol. 304 (2), pp. 31–6.
33. A. Yazawa and Y. Takeda: *Trans. Jpn. Inst. Metals*, 1982, vol. 23 (6), pp. 328–33.
34. F. Kongoli, I. Mcbow, and A. Yazawa: *Proceedings of Sohn International Symposium on Advanced Processing of Metals and Materials*, Warrendale, PA, 2006, pp. 69–87.
35. A. Yazawa, Y. Takeda, and S. Nakazawa: *Proceedings of the Copper 99–Cobre 99*, *The Metallurgical* Society of CIM, Phoenix, AZ, 1999, pp. 587–97.
36. C.W. Bale, E. Besisle, P. Chartrand, S.A. Decterov, G.R. Eriksson, K. Hack, I.H. Jung, Y.B. Kang, J. Melancon, A.D. Pelton, C. Robelin, and S. Peterson: *CALPHAD*, 2009, vol. 33, pp. 295–311.
37. FactSage™ 6.4: www. Factsage.com. Accessed August 2015.
38. Y. Takeda, S. Ishiwata, and A. Yazawa: *Trans. Jpn. Inst. Metals*, 1983, vol. 24 (7), pp. 518–28.
39. W.X. Yan, D. Lian, D. GuiFang, W. Peng, W. Wei, W. Liduo, and Q. Yong: *Chin. Sci. Bull.*, 2009, vol. 54, pp. 2810–13.
40. M. Balkanski, M.A. Nusimovici, and J. Reydellet: *Solid State Commun.*, 1969, vol. 7, pp. 815–18.
41. M. Micoulaut, L. Cormier, and G.S. Henderson: *J. Phys. Condens. Matter.*, 2006, vol. 18, pp. R753–84.
42. Handbook of Minerals Raman Spectra (ENS-Lyon): Free Database 2000-2015 http://www.ens-lyon.fr/LST/Raman. Accessed August 2015.
43. J.H. Park and D.J. Min: *Metall. Mater. Trans. B*, 1999, vol. 30B, pp. 689–94.
44. O.M. Sreedharan, E. Athiappan, R. Pankajavalli, and J.B. Gnamoorthy: *J. Less-Common Metals*, 1979, vol. 68, pp. 143–52.
45. G. Sodeck, P. Entner, and A. Neekel: *High Temp. Sci.*, 1970, vol. 2, pp. 311–21.
46. J.P. Hager, S.M. Howard, and J.H. Jones: *Metall. Trans.*, 1973, vol. 4, pp. 2383–88.
47. G.K. Sigworth and J.F. Elliott: *Can. Metall. Q.*, 1974, vol. 13 (3), pp. 455–61.
48. A. Yazawa and T. Azakami: *Can. Metall. Q.*, 1969, vol. 8 (3), pp. 257–61.
49. C.B. Alcock, R. Sridhar, and R.C. Svedbergs: *J. Chem. Thermodyn.*, 1970, vol. 3, pp. 255–63.
50. J. Wang, S. Jin, C. Leinenbach, and A. Jacot: *J. Alloys Compd.*, 2010, vol. 504, pp. 159–65.

51. J.A. Duffy and M.D. Ingram: *J. Non-Cryst. Solids*, 1976, vol. 21, pp. 373–410.
52. J.A. Duffy and M.D. Ingram: *J. Phys. Chem. Glas.*, 1975, vol. 16, pp. 119–23.
53. J.A. Duffy, M.D. Ingram, and I.D. Sommerville: *J. Chem. Soc. Faraday Trans. I*, 1978, vol. 74, pp. 1410–19.
54. J.D. Gilchrist: *Extraction Metallurgy*, 3rd ed., Pergamon Press, London, 1989, pp. 198–200.
55. D.R. Ride (ed.): *Handbook of Chemistry and Physics*, 84th Ed., CRC Press, Boca Raton, FL, 2003. Table-12:14-12:15.
56. L. Pauling: *The Nature of the Chemical Bond and the Structure of Molecules and Crystals*, 3rd ed., Cornell University Press, New York, 1965.